Supplementary Information

Insight into the role of reduced graphene oxide for enhancing photocatalytic hydrogen evolution in disordered carbon nitride

Mohammad Z. Rahman, Partha Maity*, Omar F. Mohammed, Jorge Gascon,**

KAUST Catalysis Center (KCC), Division of Physical Sciences and Engineering, King Abdullah University of Science and Technology, Thuwal 23955-6900, Kingdom of Saudi Arabia

*Corresponding authors: jorge.gascon@kaust.edu.sa; mohammadziaur.rahman@kaust.edu.sa; partha.maity@kaust.edu.sa

Synthesis of d-CN and d-CN/rGO

Reduced graphene oxide (rGO) was purchased from Sigma Aldrich, and used as received. The d-CN was prepared from thiourea and dicyandiamide by mixing at a weight ratio of 10:1. The mixed precursor was heated for 4 h at 650 ^{o}C with a ramp of 2.0 ^{o}C/min under N_2 flow in a tube furnace. To synthesize d-CN/rGO, 10 g of thiourea and dicyandiamide (10:1) was grinded with 1 g of rGO powder, and then dissolved the mixture in DI water. The suspension was left for stirring at 90 ^{o}C until the water evaporated completely. Then the solid mix was subjected to heating for 4 h at 650 ^{o}C with a ramp of 2.0 ^{o}C/min under N_2 flow in a tube furnace.

Physical characterization

The crystal structure was characterized by X-ray diffraction (XRD) using a powder X-ray diffractometer (Miniflex, Rigaku) at 40 kV and 15 mA with Cu Kα radiation (λ = 0.154178 nm). The Fourier transform infrared (FTIR) spectrum was recorded on a FTIR spectrometer (Nicolet 6700). XPS analysis was carried out on an AXIS ultra-spectrometer (Kratos Analytical Ltd, GB) with monochromatic Al Kα radiation at a pressure of *ca.* 5×10^{-9} Pa. Raman spectra were collected using an iHR550 Raman microscope (HORIBA scientific) with 600 g mm^{-1} gratings and 532 nm solid lasers for excitation. Optical properties were analyzed from the UV-Vis diffuse reflectance spectra (DRS) using a UV-Vis spectrophotometer (UV2600, Shimadzu, Japan) in the wavelength of 200 to 800 nm at RT.

Photocatalytic H_2 production setup

50 mg of the photocatalyst was dispersed in 80 mL of 10 vol% triethanolamine (TEOA) in a Pyrex flask. Anaerobic conditions were maintained by sealing the openings of the flask with silicone rubber-septa. The suspension was thoroughly degassed with Ar for 30 min. A xenon (Xe) arc lamp (with an intensity 300 W cm^{-2}) with a cut-off filter ($\lambda > 420$ nm) was used to achieve visible-light irradiation. The rate of H_2 evolution was determined by sampling 0.4 mL of gas intermittently each hour through the septum of an online gas chromatograph (GC) (Clarus 480, PerkinElmer, USA). The GC was equipped with a thermal conductive detector (TCD) with a 5 Å molecular sieve column and Ar as the carrier gas. The reactor was kept under continuous stirring to prevent sedimentation of the photocatalyst during H_2 production. Deionized water was used to rinse glassware prior to experiments. Experiments were carried out at ambient temperature and pressure.

Electrochemical measurements

The working electrode was prepared by grinding 0.1 g of the photocatalyst with 0.03 g of polyethylene glycol (PEG) in 0.5 mL of ethanol to make a slurry. Using a doctor-blade method, the slurry was then coated on the fluorine-doped tin oxide (FTO) glass electrode (3 cm^2) and dried in an oven at 350 °C for 30 min under a N_2 gas flow. Electrodes coated with slurry had a measured film thickness of around 10 to 11 µm. The active area of the electrode was about 1.35 cm^2. The photocurrent measurements were performed in a three-electrode system using an electrochemical station (CHI 650D instruments) where the sample coated FTO was used as a working-electrode, Pt as a counter, and Ag/AgCl as a reference-electrode. During photocurrent measurements, sample was irradiated by a 300 W Xe arc lamp and 0.2 M Na_2S + 0.05 M Na_2SO_3 aqueous solution was used as the electrolyte.

Time-resolved PL measurements

Time-resolved PL measurements were performed using the time-correlated single-photon counting (TCSPC) and Fluorescence upconversion technique. In the present work, 370 nm laser pulses was used as the excitation light sources and a TBX-04 detection module coupled with a special Hamamatsu PMT was used for photons detection. The excitation pump pulses was generated after passing through a fraction of 800 nm beam into the spectrally tunable (240−2600 nm) optical parametric amplifier (Newport Spectra-Physics). The photoluminescence (PL) from the d-CN and d-CN/rGO were collected with a pair of parabolic mirrors (unwanted excitation light was removed by introduced selective filters) and the PL decays were detected at maxima of the steady state PL curve.

The fluorescence up-conversion measurements were carried in a Halcyone spectrometer (Ultrafast Systems), which connected to a parametric optical amplifier (Newport, Spectra-Physics) that pumped with an amplified laser system (Astrella, 800 nm, 7 mJ/pulse, 100 fs, 1 kHz, Coherent). The collected PL and the fundamental beam (800 nm) were spatially overlapped and focused in a type- I β-BBO up-conversion crystal. The upconverted PL signal was optimized by adjusting the angle of phase matching. The resulting sum-frequency mixing signal was collected and focused on an optical fiber and directed to a monochromator and a PMT detector. The instrument response function (IRF) for the up-conversion experiments was determined as FWHM of 168 fs. All the decay traces were fitted using the exponential equation (t) =

$\sum_{i}^{n} \alpha_i \exp(-\frac{t}{\tau_i})$ where, I(t) is the total intensity remaining at time t. Where, α_i and τ_i are the amplitude and decay time of i^{th} component, respectively. The average lifetime of the measured samples is calculated using $\tau_{avg} = \sum_{i}^{n} \frac{\alpha_i \tau_i}{\alpha_i}$ equation.

Femtosecond transient absorption measurement

Femtosecond transient absorption (fs-TA) transient absorption spectroscopy were performed on timescales of 0.1 ps to 6 ns, which is based on a multipass amplified Ti:sapphire laser (800 nm laser pulses of 7 mJ/pulse energy of ~100 fs pulse width having 1 kHz repetition rate, Astrella from Coherent), and in conjunction with Helios spectrometers. The excitation pump pulses at 370 nm was generated after passing through a fraction of 800 nm beam into the spectrally tunable (240−2600 nm) optical parametric amplifier (Newport Spectra-Physics). The probe pulses (UV visible and NIR wavelength continuum, white light) were generated by passing another fraction of the 800 nm pulses through the 2-mm thick calcium fluoride (CaF_2) crystal. Before white light generation the 800 nm amplified pulses were passed through a motorized delay stage. Depending on the movement of delay stage, the transient species were detected following excitation at different time scales. The white light was split into two beams and focused on two fiber optics for the improvement of better signal to noise ratio. The excitation pump pulses were spatially overlapped with the probe pulses on the samples after passing through a synchronized chopper (500 Hz), which blocked an alternative pump pulses. The absorption changed (ΔA) was measured with respect to the time delay and wavelength (λ). All TA measurements were performed in presence of 10% TEOA in water.

Supplementary Note S1: PL

The structure of CN layers (synthesized at <550 ^{0}C) are formed by Triazine (heptazine) building blocks linked by the secondary amino groups.[1] Thermal exfoliation (at > 600 ^{0}C) of such a material happens due to partial cleavage of the hydrogen bonds between the CN layers that leads to the free amino groups having much greater vibrational freedom.[2, 3] The C—H and N—H bonds are known to act as effective centers for nonradiative dissipation of electronic excitation energy due to their virtue of high-frequency oscillation.[3] Therefore, thermal exfoliation are supposed to decrease markedly the photoluminescence efficiency. The cleavage of the bonds between the individual Triazine (heptazine) fragments do cause the formation of defects that participate in nonradiative recombination processes. [2, 3] This also makes cleaved triazine (heptazine) fragments susceptible to the peroxidation because of the attack of an oxygen molecule. The formation of peroxide groups also may act as recombination centers. Hybridization with graphene oxide would most likely introduce C—OH groups by overriding the peroxide groups and deplete the pendant amino groups. Evidently, the C—OH groups cannot act as electron traps and participate in nonradiative recombination.[4] It means that graphene oxide can passivate the defects in CN and leads to a decreased probability of nonradiative processes.

Supplementary Note S2: TAS

In fs-TAS measurements, photogeneration of charge carriers are obtained with excitation of a femtosecond (fs) duration optical pulse (the pump). After short temporal delay, a less powerful short pulse (the probe) is used to monitor the excited population of charge carriers. The crosscorrelation of the pump and probe pulses determines the temporal resolution. The time delayed (between pump and probe) changes in the detected signal of the probe pulse carry the information of the excited carriers dynamics. Probing the ultrafast excited states dynamics, TA measurements is incomparable in terms of high temporal resolution that few other techniques can afford.

Supplementary Note S3: Electron-phonon coupling

According to the Born−Oppenheimer approximation, the electronic wave functions depend on the nuclear coordinates, while the faster-moving electrons produce the potential energy for nuclear motion.[5] Therefore, the interdependence of the energy difference between the electronic states and the displacement of the nuclei along a phonon coordinate results in an electron−phonon coupling. [6] The magnitude and frequency of electron–phonon coupling influence the rates and pathways of the electronic relaxation process after an optical excitation, and greatly contributes to the time scales and efficiencies of interfacial charge separation and the transfer. [5, 7] The electron–phonon interaction therefore limits the lifetime of excited electrons or holes.[7]

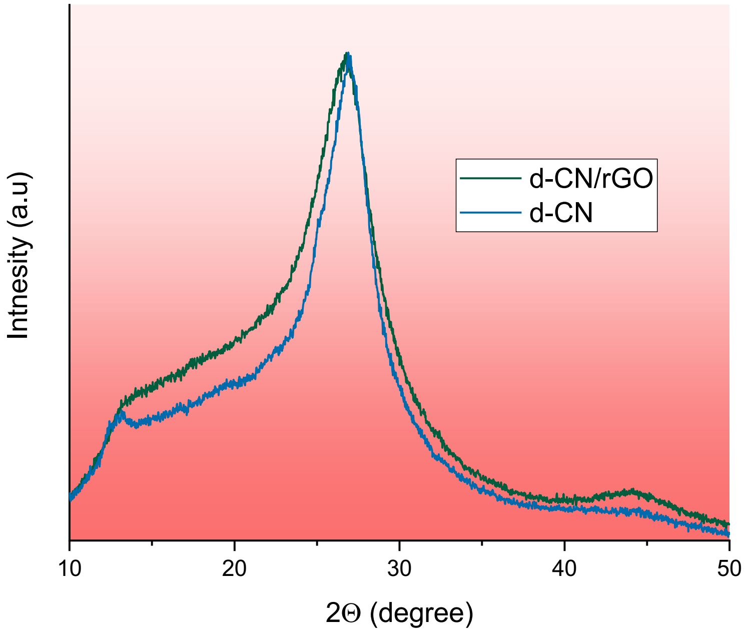

Fig. S1 XRD diffractogram. Compared to d-CN, the XRD pattern of d-CN/rGO shows a relatively flat peak at ~13° that describes the in-plane structural packing motif and a broader inter-planar stacking peak at ~27.0°. These are the characteristic peaks observed in polymeric carbon nitrides. It suggest that rGO is not incorporated to the lattice but connected to terminal groups of carbon nitride moieties.[2, 8]

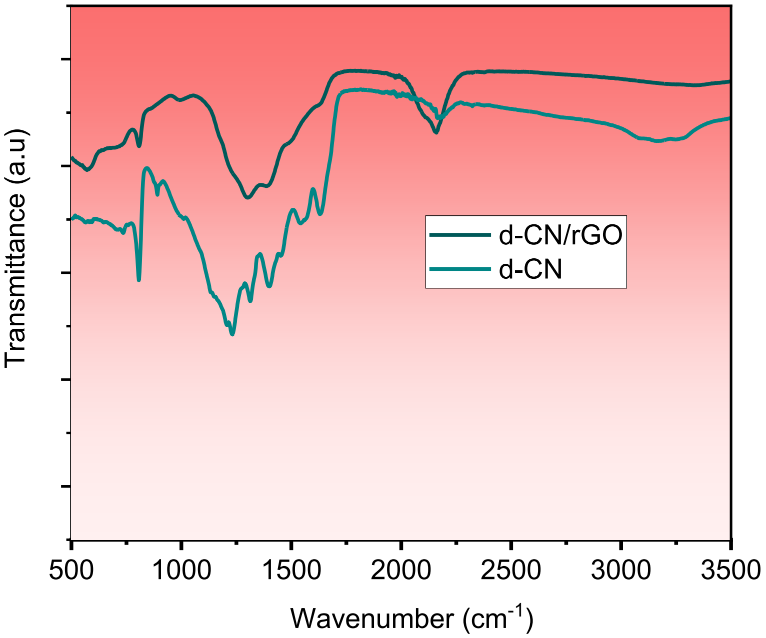

Fig. S2 FTIR spectra. In this FTIR spectra, the C–O stretching vibrations of epoxy groups at 1096 cm^{-1} and C═O stretching vibrations of COOH groups at 1725 cm^{-1} for rGO are absent in the d-CN/rGO, except typical C–N heterocycles (C–N, C═N) at 1000 to 1500 cm^{-1}.[9]

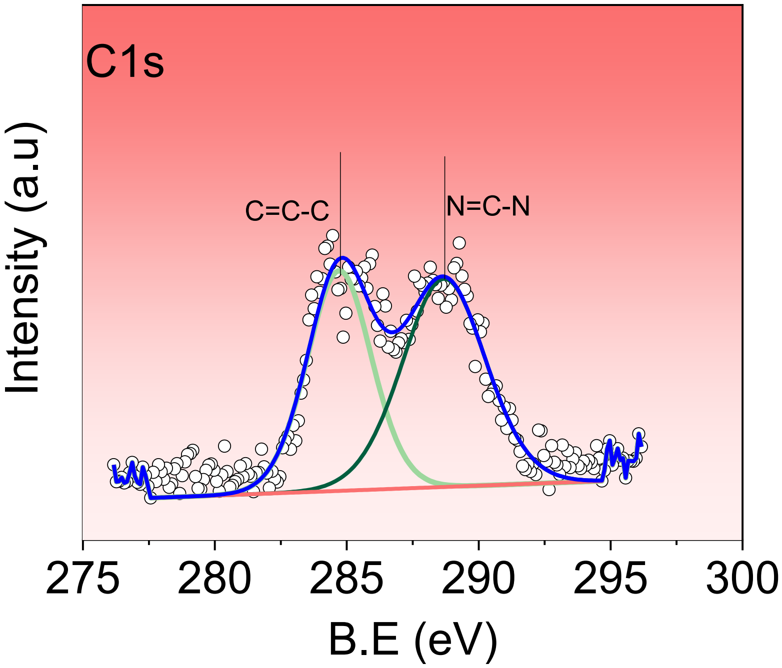

Fig. S3 XPS deconvoluted C1s spectrum that consists only of C═C–C and N═C–N groups.[10]

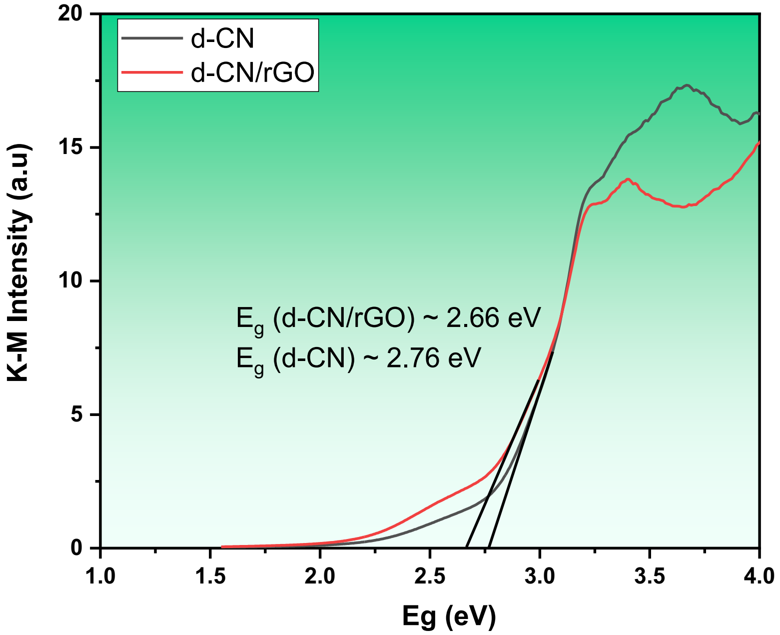

Fig. S4 Kubelka-Munk (K-M) plot for extrapolating bandgap. An indirect transition for the absorption spectra has been assumed.

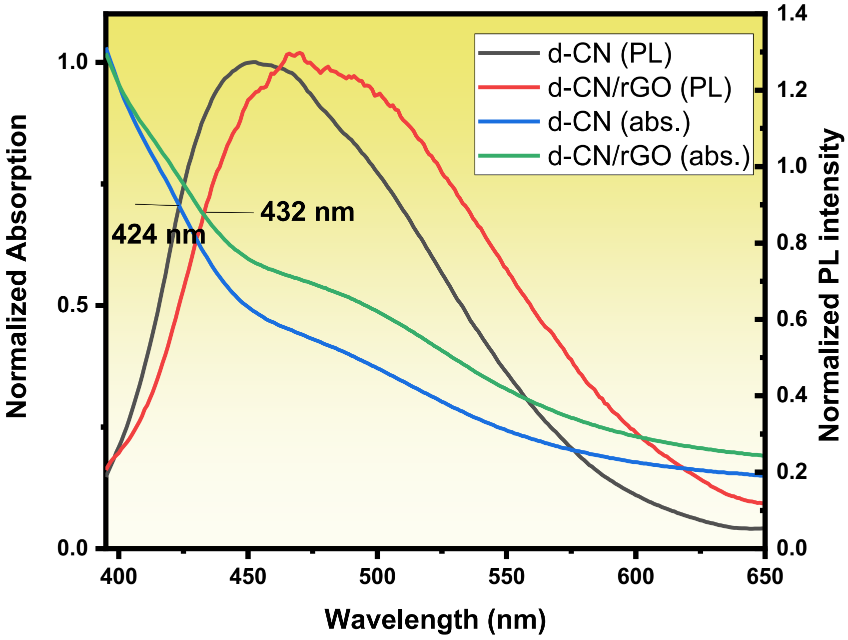

Fig. S5 Combined UV-Vis and PL spectra.

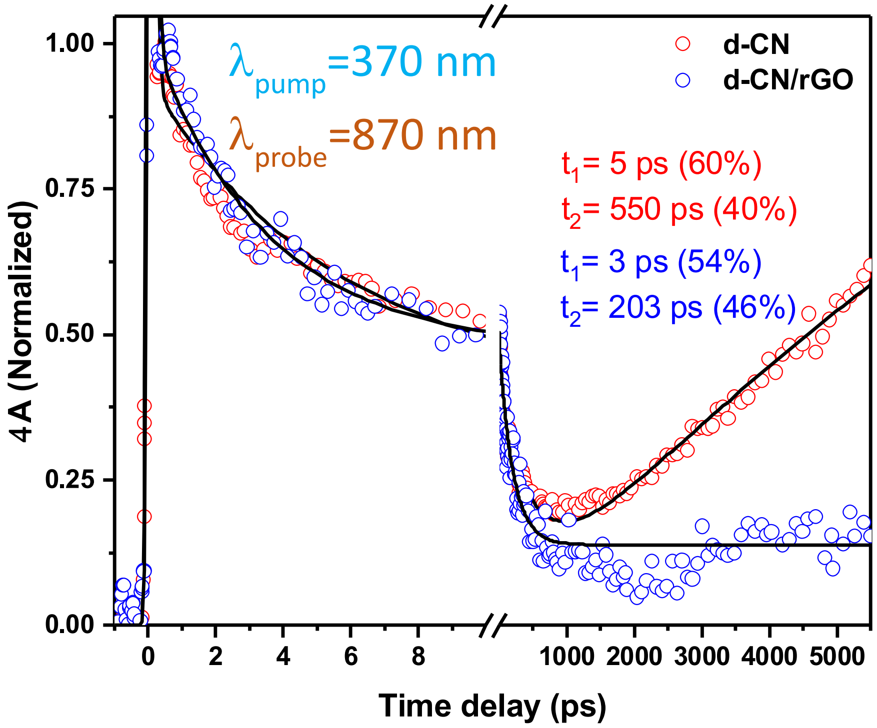

Fig. S6 Normalized TA kinetics of d-CN and d-CN/rGO at 870 nm following 370 nm excitation. Black solid lines represent the exponential fitting of the experimental data.

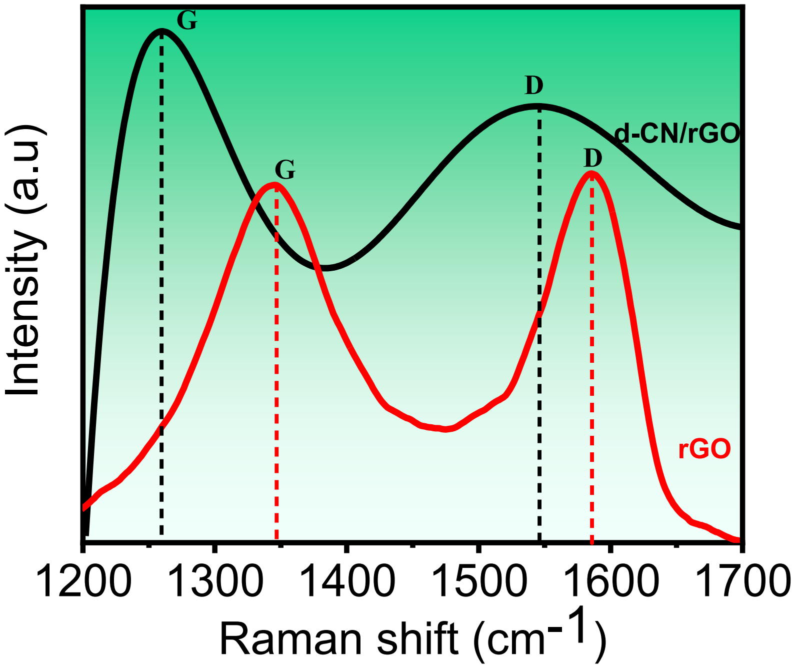

Fig. S7 Combined Raman spectra showing typical D and G band in d-CN/rGO that confirm the incorporation rGO into the d-CN skeleton.[11]

References

1. M. Z. Rahman, K. Davey and C. B. Mullins, *Adv. Sci.*, 2018, **5**, 1800820.
2. M. Z. Rahman, P. C. Tapping, T. W. Kee, R. Smernik, N. Spooner, J. Moffatt, Y. Tang, K. Davey and S.-Z. Qiao, *Adv. Funct. Mater.*, 2017, **27**, 1702384.
3. Y. Kang, Y. Yang, L. C. Yin, X. Kang, L. Wang, G. Liu and H. M. Cheng, *Adv. Mater.*, 2016, **28**, 6471-6477.
4. A. L. Stroyuk, Y. V. Panasiuk, A. E. Raevskaya and S. Y. Kuchmy, *Theor. Exp. Chem.*, 2015, **51**, 243-251.
5. B. K. Ridley, in *Hot Carriers in Semiconductor Nanostructures*, ed. J. Shah, Academic Press, San Diego, 1992, DOI: https://doi.org/10.1016/B978-0-08-092570-7.50007-6, pp. 17-51.
6. A. M. Kelley, *J. Phys. Chem. Lett.*, 2010, **1**, 1296-1300.
7. P. Hofmann, I. Y. Sklyadneva, E. D. L. Rienks and E. V. Chulkov, *New J. Phys.*, 2009, **11**.
8. F. K. Kessler, Y. Zheng, D. Schwarz, C. Merschjann, W. Schnick, X. Wang and M. J. Bojdys, *Nat. Rev. Mater.*, 2017, **2**, 17030.
9. Y. Hou, Z. Wen, S. Cui, X. Guo and J. Chen, *Adv. Mater.*, 2013, **25**, 6291-6297.
10. D. Li, M. B. Muller, S. Gilje, R. B. Kaner and G. G. Wallace, *Nat. Nanotechnol.*, 2008, **3**, 101-105.
11. A. C. Ferrari, J. Robertson, A. C. Ferrari and J. Robertson, *Phil. Trans. R. Soc. A*, 2004, **362**, 2477-2512.